Department of Energy/National Energy Technology Laboratory DOE Award Number: DE-FE0031651

Project Title: Development of a Pipe Crawler Inspection Tool for Fossil Energy Power Plants

Principal Investigator

Dwayne McDaniel, Ph.D., P.E.

Principal Scientist

(305) 348-6554

mcdaniel@fiu.edu

Co-Principal Investigator
Aparna Aravelli, Ph.D.
Research Specialist II
(305) 348-8219
aaravell@fiu.edu

Submission Date: September 6, 2022 DUNS Number 071298814

Recipient Organization: Applied Research Center Florida International University 10555 W. Flagler Street EC2100 Miami, FL 33174

> Project Period: 9/1/2018 – 8/31/22 Reporting Period End Date: 8/31/22 Final Report Signature of Submitting Official

Wayne E. Malan

CONTENTS

1. INTRODUCTION	3
2. TECHNICAL APPROACH AND RESULTS	3
2.1 Background	3
2.2 Robotic Crawler	6
2.2.1 Peristaltic Modules	6
2.2.2 Electronics and Communication System	9
2.2.3 Inspection Modules	12
2.3 Bench-Scale Testing	18
2.3.1 Robotic Crawler	18
2.3.2 Ultrasonic Transducer Module	19
2.3.3 Instrumentation Module	20
2.4 Engineering-Scale Testing	21
2.5 Simulation Model Development	24
2.6 Simulation in ADAMS	27
3. CONCLUSIONS	33
4. PARTICIPANTS AND OTHER COLLABORATING ORGANIZATIONS	34
5 REFERENCES	35

1. INTRODUCTION

This document presents the final report of the research activity completed during the four years of the project and includes the major challenges and accomplishments. The report presents specific details of the engineering processes and methodologies used to develop the robotic crawler and complete the project milestones. In particular, the report includes sections that address the problem statement, background, development of crawler modules, bench scale testing, simulation development and full scale testing. The report concludes with a discussion on potential paths forward and concluding remarks.

2. TECHNICAL APPROACH AND RESULTS

This section contains the approach utilized to develop our robotic crawler. It begins with a section on the motivation and background of the research and is followed with a description of our approach to address the issues. The development of the crawler motion modules is then discussed with descriptions of the electronics and communication. This is followed by the development of the inspection modules and bench scale testing. Two crawlers are then developed and demonstrated in an engineering scale testbed. Finally, the development of a high fidelity virtual simulation model of the crawler is presented with a discussion on the challenges and results.

2.1 Background

The power generation of a superheater power plant relies on burning coal to boil water and convert it to steam. The superheated steam, produced in the combustion chamber, is directed to the turbines of the plant to generate electricity by converting the kinetic energy of the fluid into electrical energy. The combustion chamber contains numerous pipes, typically found in a coiled structure, that operate at temperatures up to 540° C and pressures between 10 to 1000 bar. In addition, the tubes range from 1.3 to 7.6 cm in diameter [1]. These tubes are located in the hottest region of the steam generator and can fail if maintenance and inspections are conducted infrequently. Prolonged operation can result in the rupture of critical components, stemming from plastic deformation and surface oxidation [2].

To avoid failure, an inspection of the superheater tubes should be done periodically. Typically, these inspections are conducted externally, and are often manual and time-consuming. They are also challenging, as some areas are difficult to reach, and the environment can be dangerous for humans. Recently, robotic inspections have seen an increase in utilization as an alternative to human-based examinations [3]. One approach using robotic inspections is to conduct the evaluation on the external surface of the pipes or tubes [4]. These devices [5, 10] crawl on the external surface of the tubes using different adhesion mechanisms including suction [8], thrust propellers, and magnets [9]. These systems can detect pinholes, cracks, and thickness reduction due to erosion and corrosion using sensors such as electromagnetic acoustic transducers [10] and other non-destructive tools.

Although some of the technical issues with external systems have been addressed, there are still some challenges that need to be investigated. This includes the potential difficulty of navigating on pipes with limited external access. An example includes boiler superheater tubes that are often stacked and don't allow for the external inspection of the tubes inside the combustion chamber. Internal inspection systems offer an alternative to the more conventional external approach. These systems do not have issues with the external constraints but have their own challenges due to the reduced availability of space. They also can require the system to be shut down prior to the inspection. Several designs and concepts for in-pipe inspection systems have been discussed in the literature [11, 22]. These systems perform a variety of tasks including internal cleaning of ducts [17], measurement of surface thickness, mapping of tubes, and visual inspection [18].

One of the significant challenges for internal crawler systems is the ability to generate traction within the limited space of the tubes. Earthworm type robots [19, 20] offer larger traction output but require several degrees-of-freedom. Wheeled [21] and treaded [22] systems offer simpler designs but generate less traction. The compromise between maneuverability and design simplicity is a major challenge in developing a robotic inspection system. There is little research that has been conducted on the development of internal crawlers for superheater tubes and small diameter pipes, in general. This is likely due to the limited space available and the coiled nature of the tubes.

This project aimed to create a novel robotic inspection tool that can navigate through small diameter pipes and provide information on the structural integrity of tubes typically found in powerplant superheaters. The system consists of a tethered pipe crawler that can navigate through the coiled tubes with 180° bends and diameters as small as 5 cm. The primary crawler will contain modules that house inspection sensors including a LiDAR, environmental sensors, cameras, and an ultrasonic gauge for measuring the tube thickness. Multiple auxiliary crawlers will also be utilized for load distribution of the tether as the system navigates through the multiple bends and straight sections. A schematic of the concept is shown in Figure 1.

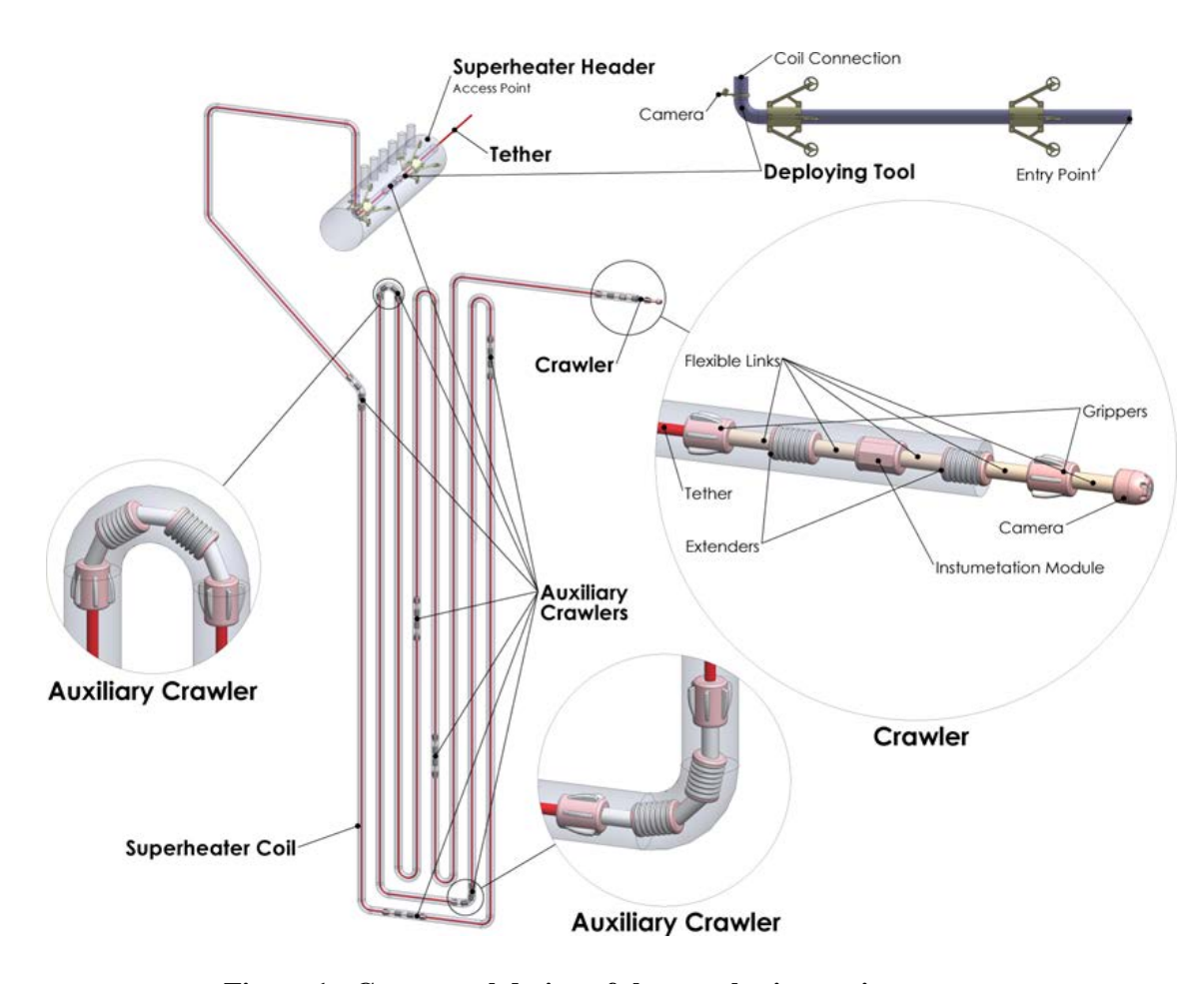


Figure 1 - Conceptual design of the crawler inspection system.

2.2 Robotic Crawler

The robot is modular and consists of several segments, which are 3-D printed and use offthe-shelf components. Some machined and metal parts are also included to increase the mechanical efficiency and improve the robot's reliability. Below is a description of each modular segment of the robot.

2.2.1 Peristaltic Modules

Movement of the crawler is generated using a set of gripper and extender modules that propel the crawler forward using peristaltic motion, similar to earthworms that travel by contracting their body segments sequentially. Each module holds a linear actuator consisting of a rotating lead screw and nut. The basic design is composed of five modules: two grippers, one at the front and one near the rear of the system, two extenders, between the grippers and one electronics module. The modules are connected via a flexible cable that has the strength to handle the push/pull loads and is also flexible enough to allow for significant rotation between the modules. The peristaltic movement of the crawler is shown in Figure 2.

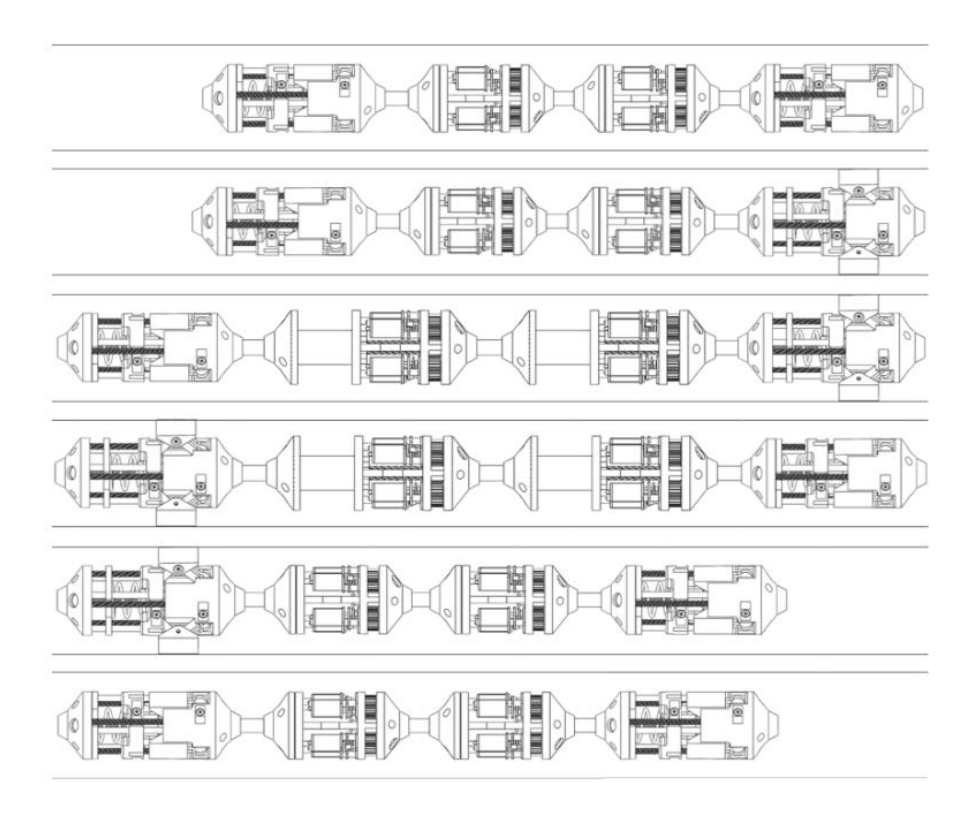


Figure 2 - Peristaltic motion of the crawler.

The gripper module has three pads to hold into the pipe wall. The pads are connected to a moving disk and the module's base. The moving disk has a central hex nut, which transforms the rotational movement of the lead screw to the linear movement of the disk. The pads open and close perpendicular to the tube wall with the movement of the disk. A metal gear motor installed on the module's base actuates the lead screw. Figure 3 shows the components of the gripper module.

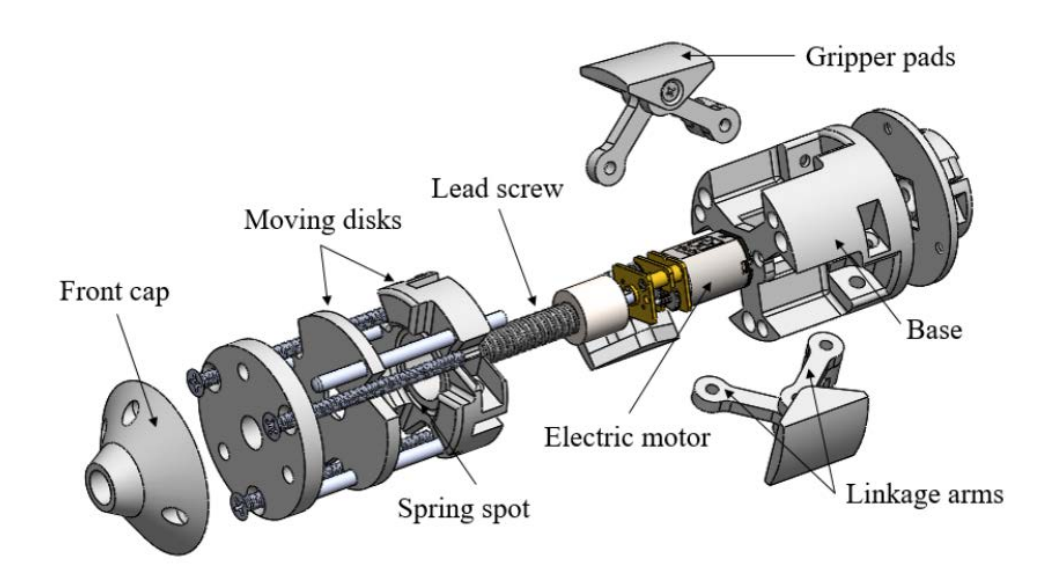


Figure 3 – Exploded view of the gripper module.

The mechanism of the gripper module can extend past the pipe wall, allowing for variations in pipe diameter. Additionally, the pads are covered with rubber for increased friction. All the parts of the crawler are 3-D printed and assembled using off-the-shelf components as screws, dowel pins, heat sets and the electric motors.

The extender module utilizes a lead screw to generate the linear motion required for the peristaltic movement. Two electric motors drive the lead screw and these components are connected by a set of gears located on the module's base. A cylinder holds a hex nut that transforms the rotation of the lead screw to linear movement to the cylinder. The cylinder then propels the front cap of the module, generating the motion. Figure 4 shows the design of the module, highlighting some of its components.

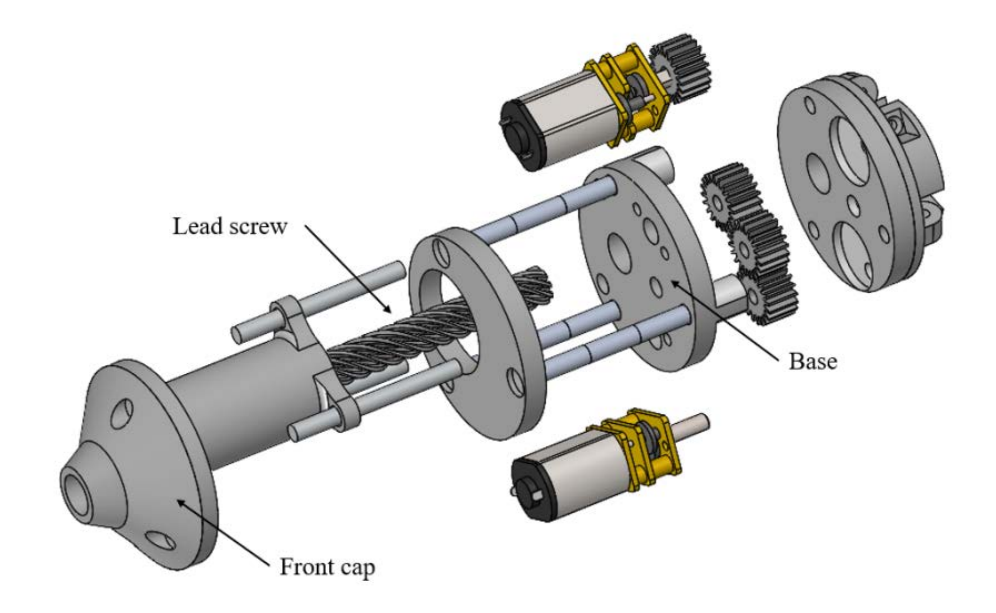


Figure 4 – Exploded view of the extender module.

The reduction rate of the motors and the travel distance per turn of the leadscrew directly affect the crawler's velocity and pull force capabilities. Therefore, the optimal combination of those components leads to an increased payload and faster travel per cycle. Several combinations of motors and leadscrew were tested during the development of the extender module. The one that best facilitated the projects' requirements used a reduction rate of 298:1 for the electric motor and the fast lead screws, with a travel distance of 8.45 mm per turn.

The extender module utilizes some metal components to increase the overall accuracy. As an example, the metal gears fit without any gaps. This efficiency would be difficult to achieve by 3D printing such small components. Other metal components being used include dowel pins, heat set, and the lead screw. In addition, a printed circuit board (PCB) was designed to Y-cable the electric motors. The board also assists in replacing the electric motors if a malfunction is detected.

The selection of actuators was critical to the design of the crawler. The choice of electric linear actuators versus pneumatic actuators involved consideration of several factors. Reliance on compressed air throughout the crawler posed a challenge in the tether design management. Additionally, electric motors are much smaller and require thinner wiring than the pneumatic motors. It should be noted that there was a clear trade-off between reducing the module's overall dimensions versus simplifying the system's overhaul control. Pneumatic actuators provide a much simpler method of producing linear motion.

A stabilization system was designed to maintain balance during circumferential rotations, and it is incorporated in all modules. It integrates a set of lever arms mounted on three separate linkages, which are connected to a pair of springs providing consistent opposing force to a set of wheels, mounted on the outer extremity of the arm. The applied force offsets gravity during the rotation of the module, establishing continuous surface contact for each of the wheels during rotation. This mechanism allows the module to conform to the pipe surface in minor irregularities while maintaining precise placement.

A high resistance flexible tube attached to the rear end of each module provides the stiffness required but is also flexible enough to allow movement around the bends. In addition, the rear stabilization system provides enough stability for the module it is attached to and the unit following it. This allows both units to remain centered within the pipe. The tubes also house the wiring required for power and signal lines.

2.2.2 Electronics and Communication System

The challenge for the controls of the system was addressed in developing the electronics and communication system for the crawler. A module has been incorporated that houses the major electronic components. This includes the embedded microcontroller, voltage regulator, current sensors, and motor controllers that are mounted onto printed circuit boards. The electronics module was added to the rear end of the peristaltic crawler and controls the movement of each gripper and extender, as seen in Figure 5.

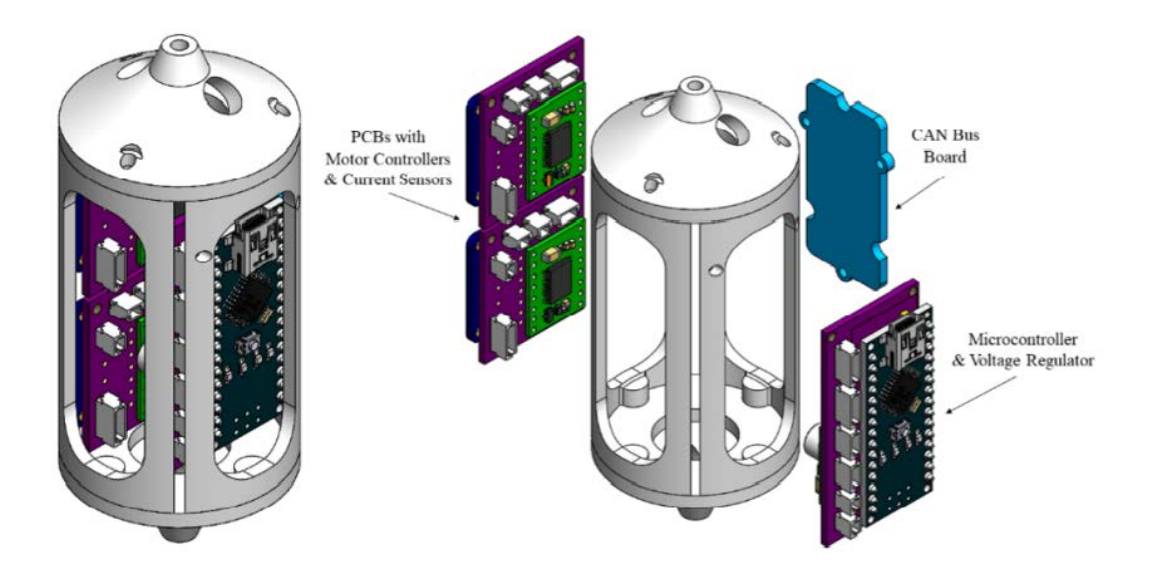
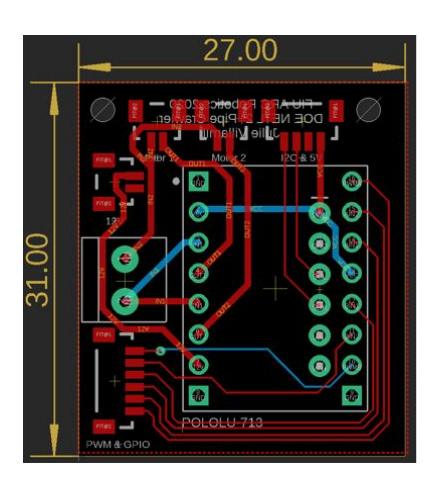


Figure 5 - Electronics module.

The electronics module contains several custom designed printed circuit boards (PCBs) that combine the components. During the design process, several options were considered for the module. The first option included building an arrangement of breakout boards stacked together inside each module. To simplify the soldered connections in the design, an alternative option was implementing two PCBs to mount the breakout boards together. These components control the movement of each module through I2C communication protocol. The second board (right) contains the main microcontroller, voltage regulator, and connections to a separate board containing the communication system. A challenge in developing the electronics module was the compact arrangement of the wires. Efforts were focused on designing the boards with plastic JST connectors to minimize the module size as much as possible. Figure 6 shows the schematics of the two PCBs developed for the electronics module.



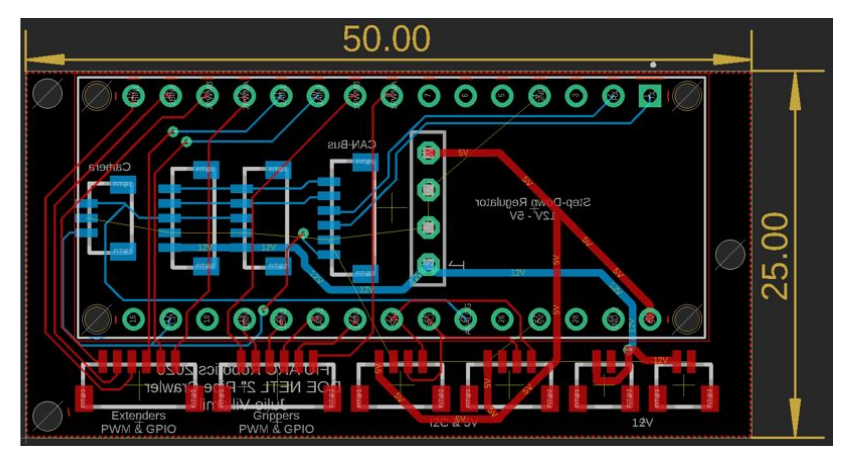


Figure 6 - Custom printed circuit boards.

The tether connecting the modular crawlers is a significant component of the system as it is used for communication and power. It wires the multiple devices together in sequence, daisy-chaining all components, establishing intermodular communication, supplying electrical power, and providing analog video feedback to the control box. Several protocols, including RS-485, CAN Bus, and SPI, have been evaluated to provide more efficient and streamlined communication.

The design of the PCBs heavily considered the wire connections for the serial communication system. Although RS-485 serial protocol was previously investigated, CAN Bus (Controller Area Network) communication was tested using a serial CAN module compatible with Arduino. Similar to RS-485, the CAN Bus communication allows for long distance communication and is used to send and receive data between the components and an external computer. CAN Bus is a serial messaging protocol based on pairs of receivers and transceivers. It is especially useful for systems with multiple controllers and is commonly used in automobiles. In addition, it was chosen for its debugging features and error management.

The wires connecting these CAN Bus boards to the system include CAN High and Low for bi-directional data transfer and RX/TX to the Arduino microcontrollers. In addition, a challenge faced was the implementation of masks and filters which sort through the identification of each data message being transferred. The architecture of the CAN Bus communication is described in the Figure 7.

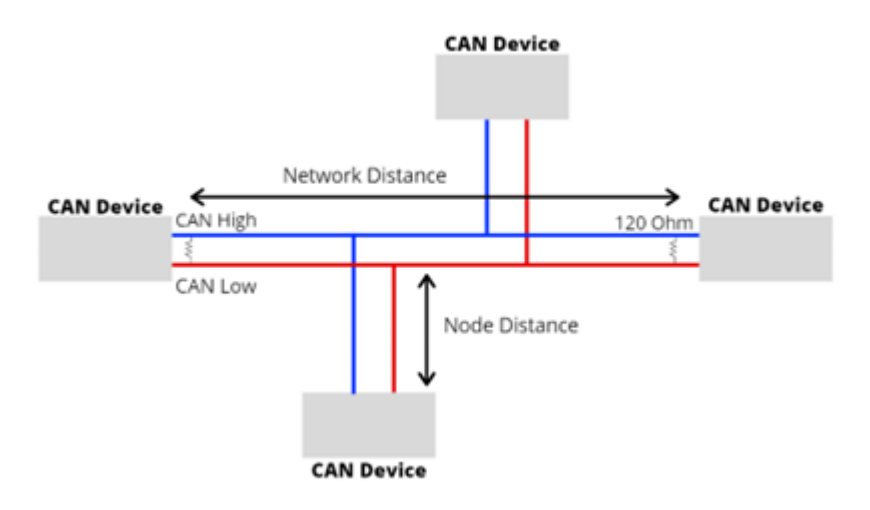


Figure 7 - CAN Bus architecture.

2.2.3 Inspection Modules

The purpose of the crawler is to provide information regarding the structural integrity of key pipeline components in fossil energy power plants. Inspection modules have been developed to house inspection sensors and are described in the following subsections.

2.2.3.1 Instrumentation Module

The instrumentation module is designed to improve the inspection tool capabilities, robustness, and operational feedback. The module consists of a rotative cylinder with a stationary top and bottom flanges. This module utilizes a spur gear mechanism to provide the rotation of the cylinder, which constantly spins 360° degrees concentrically about the center of the tube. Six plates are attached to the cylinder wall and each plate accommodates different sensors to evaluate the conditions of the tube. Each panel design can be modified to support a different sensor, varying according to each project necessities. Figure 8 shows the module's rotating drum and the motor housing, highlighting some of its components.

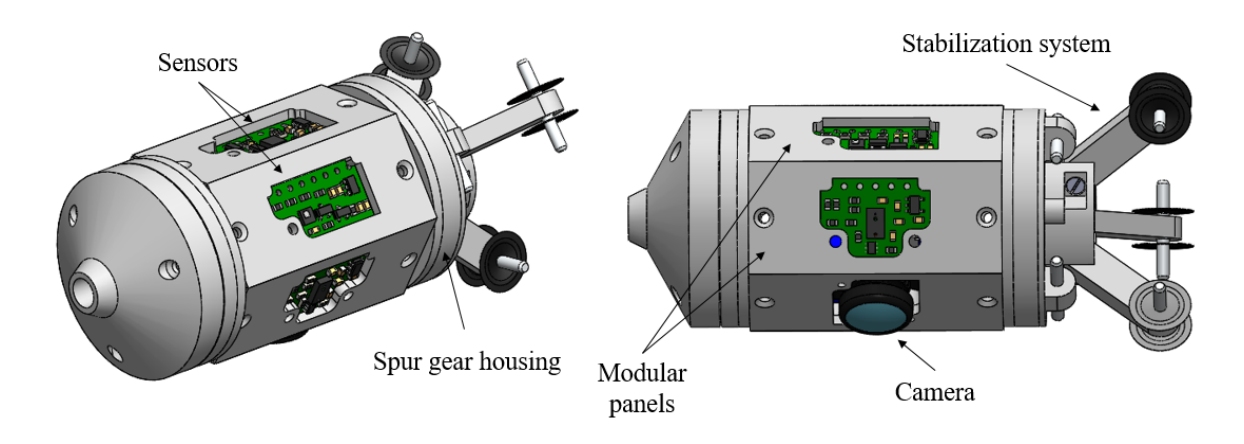


Figure 8 – Instrumentation module.

The module currently includes 3 sensors for assessing the tube conditions, although there are 3 more panels available for additional sensors in the future. The three current sensors include an analog video camera, an environmental sensor for temperature and pressure measurements, and a light detecting and ranging sensor (LiDAR). The LiDAR can provide information on potential surface anomalies and defects. An inertial measurement unit is also included in the module and provides the angular position and acceleration of the crawler. An embedded microcontroller manages the communication between the sensors and the electronics module. Table 1 shows the specifications of the sensors currently installed in the module.

Table 1 - Sensor Specifications

Sensor	Measurement	Range	Resolution	Unit
Environmental	Temperature	-40 - +85	±1	°C
	Pressure	26 - 126	±0.02	kPa
IMU	Acceleration	$\pm 2 - \pm 16$	± 0.004	g
	Angular Velocity	$\pm 125 - \pm 2000$	±10	$^{\circ}/s$
Camera	Surface Imaging	640X480	VGA	Pixel
LiDAR	Circumferential Mapping	10 - 60	±1	mm

A PCB embeds a microcontroller and a motor driver to manage the communication within the module sensors. The PCB designed uses I2C communication between the sensors and the microcontroller and incorporates JST wire connectors. The use of components available on the market includes the M2 screws and spacers that maintain the unit's rigidity. Furthermore, bearings were placed between the drum and the flanges (top and bottom) to reduce friction between the moving components.

A slip ring was developed to improve the wire management during rotation. The mechanism consists of a round PCB in the form of a disk. It utilizes the radial direction to connect two disks with exposed wires of varying radius. A flexible copper wire with a miniature metallic spherical tip connects the power and signal tracks and the brush block. The system is integrated into the front end, while the spur gear is attached in the back. Slip rings are commercially available, and a range of different diameters and types was found. However, an off-the-shelf slip ring was not available that could fit inside the 35 mm module. Thus, the mechanism was developed in house and Figure 9 shows the design created and the rings' exposed wires with the spinning copper cables soldered onto the board.

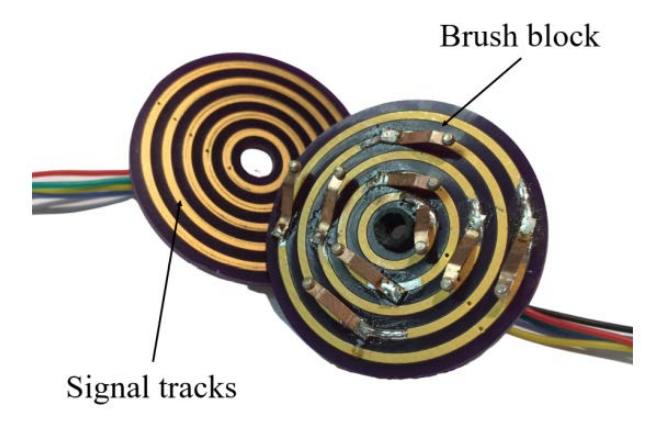


Figure 9 – Slip ring.

2.2.3.2 Ultrasonic Transducer Module

In addition to the sensors utilized by the Instrumentation module, an Ultrasonic Transducer (UT) sensor is incorporated into the crawler to improve its functionality. The module design allows the UT probe's accurate positioning on the pipe surface, providing repeated wall thickness measurements.

A linear actuator mechanism allows for the prismatic movement of the probe inside the pipe. The mechanism utilizes two plastic gear motors connected to a gearbox and a lead screw. The lead nut is attached to a housing for the UT sensor and translates along the lead screw,

converting the rotary motion from the motors to a linear motion for the sensor. A spur gear system was added to the module to allow wall thickness measurements at different circumferential spots. A stationary spur gear was mounted on the front end of the module and acts as the output shaft. The input shaft gear, connected to a plastic gear motor, spins with the module. A set of bearings permits the rotation and reduces the friction between the moving parts. This mechanism provides a full 360° rotation of the modules and allows the UT sensor to measure the tube thickness at any radial location. A schematic of the module highlighting the major components is shown in Figure 10.

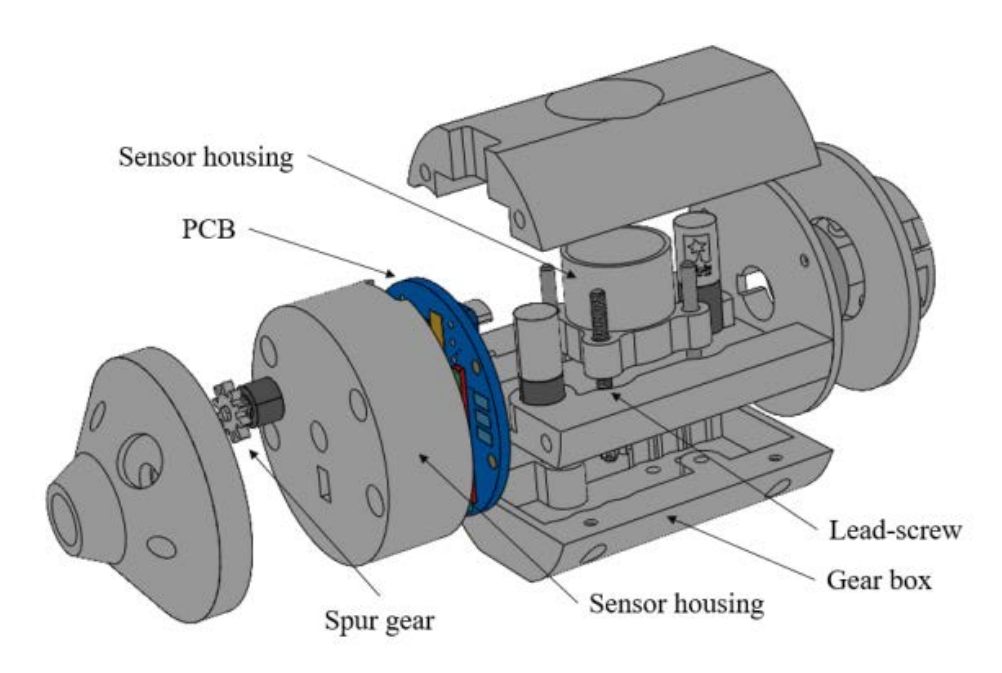


Figure 10 - UT sensor module representation.

During the development of the UT sensor module, PCBs were adapted to the constrained 35 mm diameter of the crawler. As a result, to maximize spacing for the electronics, the boards were designed to be circular. This architecture allows the circuit board to be positioned concentric inside the module, saving space compared to the traditional rectangular boards. In addition, the design contains a 6 mm hole to allow an electric motor to pass through the other side of the PCB. The PCB designed improved the integration between the UT Sensor with the other modules. This board contains a microcontroller, a dual motor controller, and a current sensor. The PCB also contains a serial port for CAN Bus communication with the electronics module and an external control box. The front end of the unit contains electronics cover where the PCB is attached.

During the evaluation of different UT sensors, it was clear that even the smallest sensor head of 7 mm used did not make significant contact with the curved internal tube surface. The small gap between the two surfaces, as shown in Figure 11, led to an offset in the thickness measurements of the 5 cm diameter tube. To evaluate the consistency of the thickness offset, a stepped steel tube section was machined to create gradually varying thicknesses along the length of the tube. The wall thickness decreased 0.198 mm at each step. Figure 11 also shows the machined tube and the thickness steps created. Thickness measurements were taken from both the inside and outside surfaces of the machined tube. Since the probe had more surface contact on the outside surface, these measurements were found to represent the actual thickness. For each thickness step, twenty measurements were obtained and averaged. The results, shown in Figure 11, were plotted with the blue line representing the measurements from the inside surface and the red line representing the measurements from the outside surface.

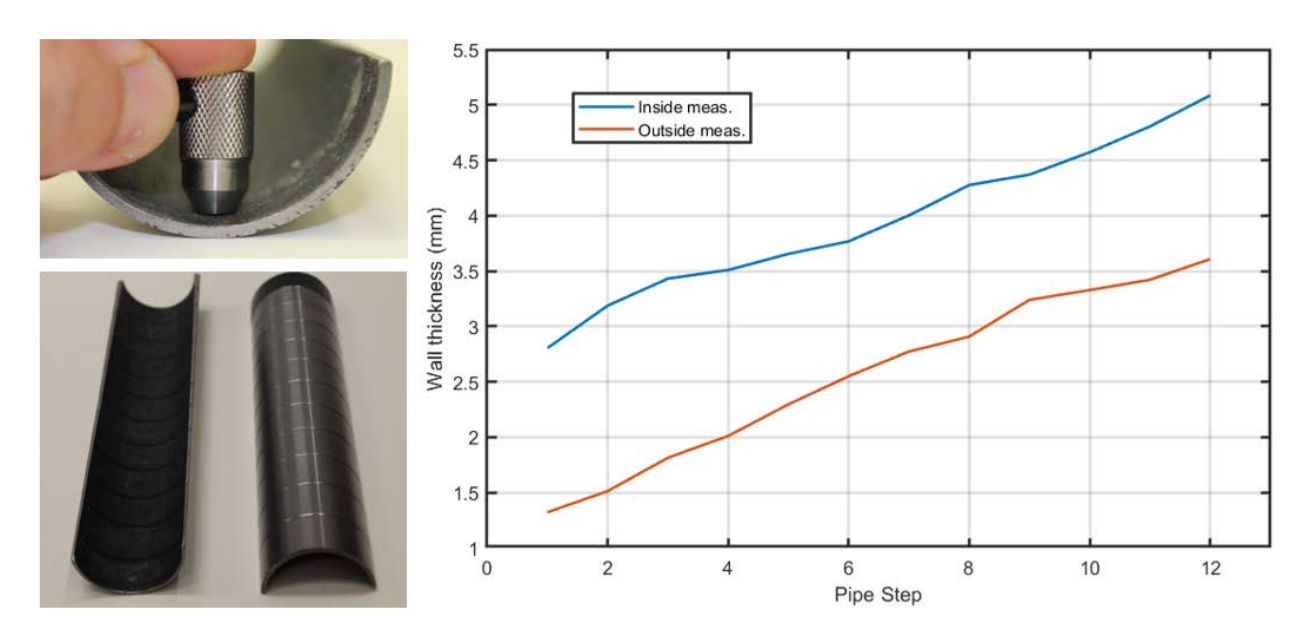


Figure 11 - Thickness measurements obtained from the inside and outside surfaces of a tube with varying thicknesses.

Several factors can affect the accuracy of measurements using a UT sensor: the angle of incidence, the couplant, diameter of the sensor head and the curvature of the pipe. Results from this analysis show that although the measurements taken from inside surfaces were off, the offset from the true thickness was fairly consistent and could be used to obtain reasonably accurate measurements.

2.2.3.3 Surface Preparation Module

The ultrasonic sensor used in the UT module requires a liquid couplant to obtain measurements. The gap between the sensor tip and the surface should be filled with a fluid to permit the ultrasonic signals to travel to and from the wall surface. Water can be used as the couplant. However, denser liquids allow for a higher refraction of the signals. Thus, a gel couplant offers a better alternative and was utilized in this system. Couplant-free ultrasonic sensors were considered for this study; however, they can require large application forces to compensate for potential gaps. Due to space limitations within the crawler, these requirements are difficult to achieve with the small electric motors currently available. In addition to the surface gap, moisture and elevated temperatures in superheater tubes increases levels of corrosion and creep in the tubes. To address these challenges, a separate module was developed for application of a gel couplant and surface-cleaning brush as shown in Figure 12.

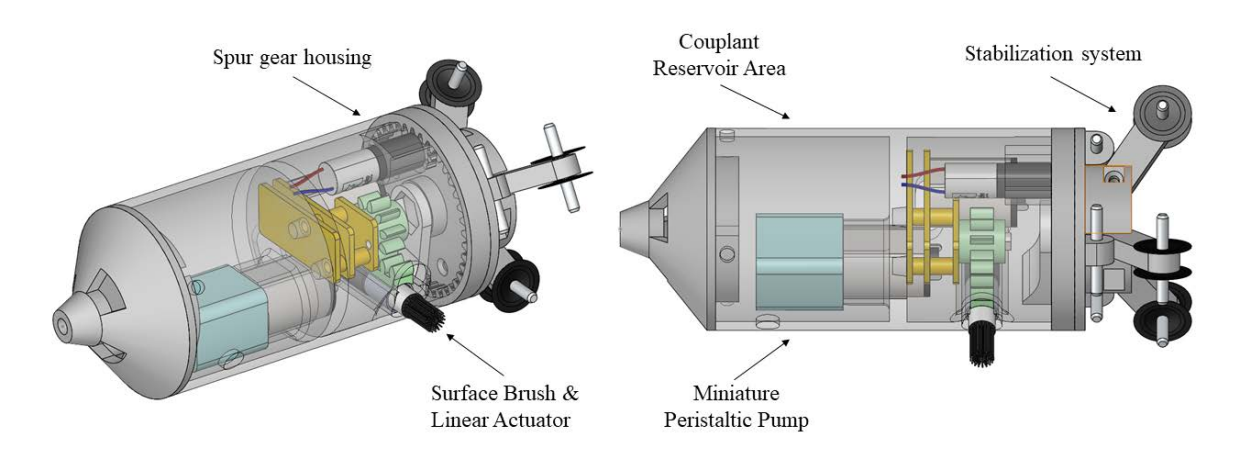


Figure 12 – Surface preparation module.

The design of the module includes four motors which rotates and extends a surface brush, drives a pump to apply a couplant, and rotates the module. To apply the gel couplant needed for the UT sensor, a peristaltic pump is used to transfer the gel from a reservoir to the tube inner surface. A chamber at the front of the module houses a reservoir containing the gel and the pump. Due to the available space in the module, the pump selected was based on its size, flow rate, pressure, and compatibility with the liquid.

A surface-cleaning brush is attached to a motor mounted perpendicular to the module. Radial extension of the brush and its motor is accomplished using a rack and pinion gear. This allows the components that make up the brush to fit within the diameter of the module. The brush can then be positioned on the tube surface for cleaning when needed.

Since the UT sensor will need to obtain measurements around the circumference of the tube, this module also contains a spur gear system for rotation. This allows the module to rotate and prepare the internal surface for measurements using the brush and couplant.

2.3 Bench-Scale Testing

The development of the crawler system started with creating general concepts and initial prototyping and proceeded with bench-scale testing and engineering-scale testing of the system. This section presents the bench-scale testing used to validate the concepts and testing of the system in a tube with multiple bends and straight sections.

2.3.1 Robotic Crawler

To evaluate the pull force capability of the crawler, pull force tests were conducted on the gripper and extender modules. The grippers were found to be capable of pulling approximately 84.5 N of force and the extenders were found to generate 40 N of force. These values demonstrate that the forces obtained in the motion analysis are reasonable approximations of the actual pull forces (discussed in a subsequent section). The pull force tests were conducted using a digital weight scale attached to the ends of the modules. The value for the gripper was found by finding the maximum pull force before the gripper pads began to slip along a steel 5 cm diameter tube. The pull force for the extender was found by clamping the module to a flat surface and allowing the module to pull the scale.

After the initial system was assembled, bench-scale tests were conducted to evaluate the crawler's ability to navigate through both straight and 180^{0} elbow sections (Figure 13). The elbow testing was conducted in a custom built 5 cm diameter tube with a 7 cm bend radius. Although the system was designed to navigate through bends with a 5 cm radius of curvature, the smallest bend radius found in a transparent acrylic pipe was 7 cm. With this experimental setup, the crawler was easily able to navigate through the bend. The average speed of the crawler in straight sections was found to be 50 cm/min. The speed was slightly slower when navigating through the bends.



Figure 13 - Robotic crawler traveling in straight tube section and plastic U-bend.

2.3.2 Ultrasonic Transducer Module

To demonstrate the functionality of the UT module, tests were performed in a clear acrylic 5 cm diameter straight tube with a wall thickness of 1.6 mm. The UT gauge was calibrated to measure the thickness of PVC by adjusting the velocity of sound to 2390 m/s. Since the module was not integrated with the crawler for the bench-scale testing, the stabilization mechanism was adapted to be used at both ends of the module. Figure 14 shows the test performed with the module. Wall thickness was measured at three different locations around the inner circumference of the tube.



Figure 14 - Measurements performed on the tube's inner surface.

The circumferential rotation using the spur gear set allowed the module to obtain measurements at different locations along the inner wall of the tube. As shown in Figure 14, the measurements were consistent between 2.5 and 2.6 mm. As noted in Section 2.3.3.2, the flat sensor head does not mate perfectly with the internal tube surface due its curvature. Thus, an offset must be subtracted from the measurement to obtain a more accurate reading.

2.3.3 Instrumentation Module

To evaluate the laser range detection sensor in the instrumentation module, a template ring was used to simulate a 5 cm diameter surface with a variety of irregularities. During the testing, the module is positioned at the center of the template frame and rotates to scan the surrounding irregularities on the ring. Figure 15 shows the template ring and the instrumentation module positioned at the center.

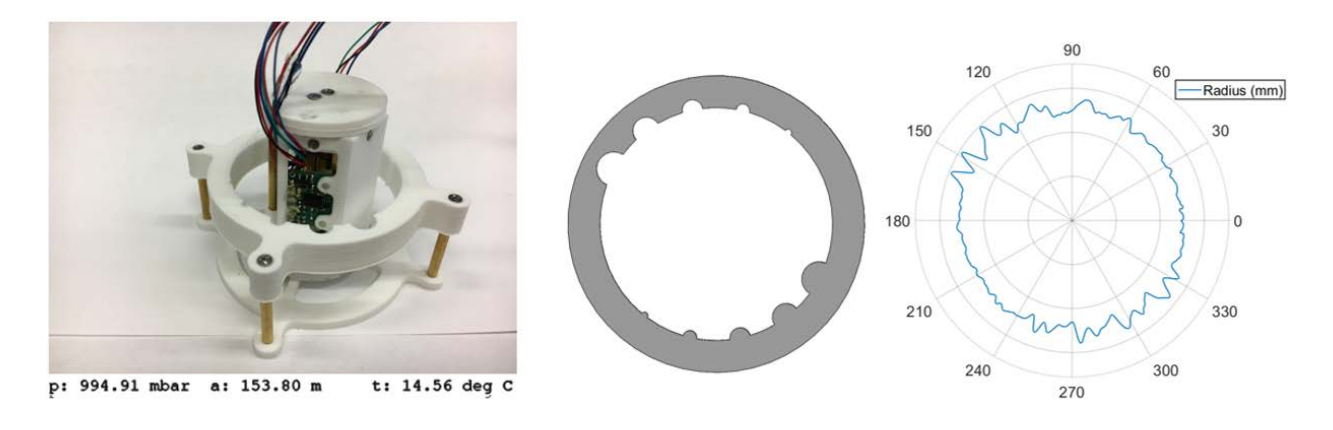


Figure 15 - Instrumentation module testing.

Preliminary results demonstrate the potential for the detection of anomalies in tubes and pipes using the VL6180X LiDAR sensor. Data from the environmental sensor is also shown and

includes pressure (p), altitude (a), and temperature (t). It should be noted that the camera was not installed during this testing.

2.4 Engineering-Scale Testing

To evaluate the crawler's performance in a larger scale testbed, a mock-up similar to the superheater tubes found in fossil energy power plants was constructed. The testbed was manufactured with acrylic plastic tubes so the crawler could be observed while navigating through the straight sections and 180° elbows. As shown in Figure 16, the crawler was able to navigate through multiple straight pipe sections and bends and was only limited by the length of the tether.

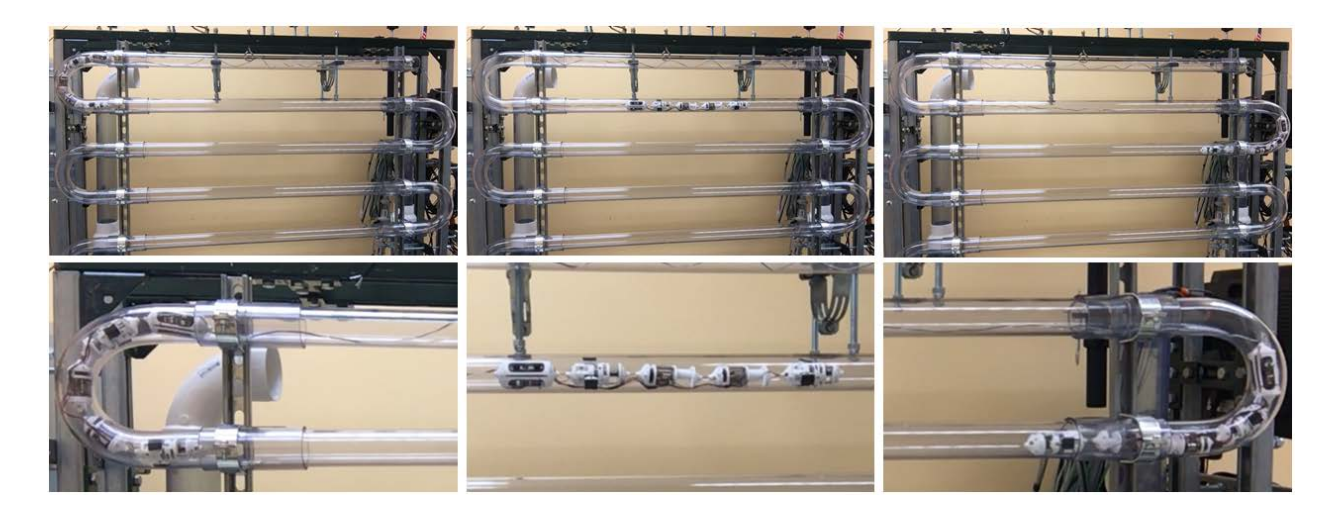


Figure 16 - Crawler navigating the superheater tube mock-up with magnified images.

Testing was also conducted to determine how the tether load changes as the crawler navigates through multiple bends and straight sections. The testing included passing a tether through the tubes and measuring the load after each 180° bend. Measurements were taken using a digital scale and repeated 7 times after each bend. Figure 17 shows a graph with the blue line representing the tether load averaged after each bend (x-axis on the graph).

It can be noted from Figure 17 that the tether load increases significantly after the fourth bend. The tether load average was 42.5 N after the 4th bend and was 132.3 N after the 5th bend. This represents an increase of 311% in tether load. Since the crawler pull force is approximately 40 N, it is expected that the crawler can navigate through three bends before needing an additional crawler to assist in pulling the tether.

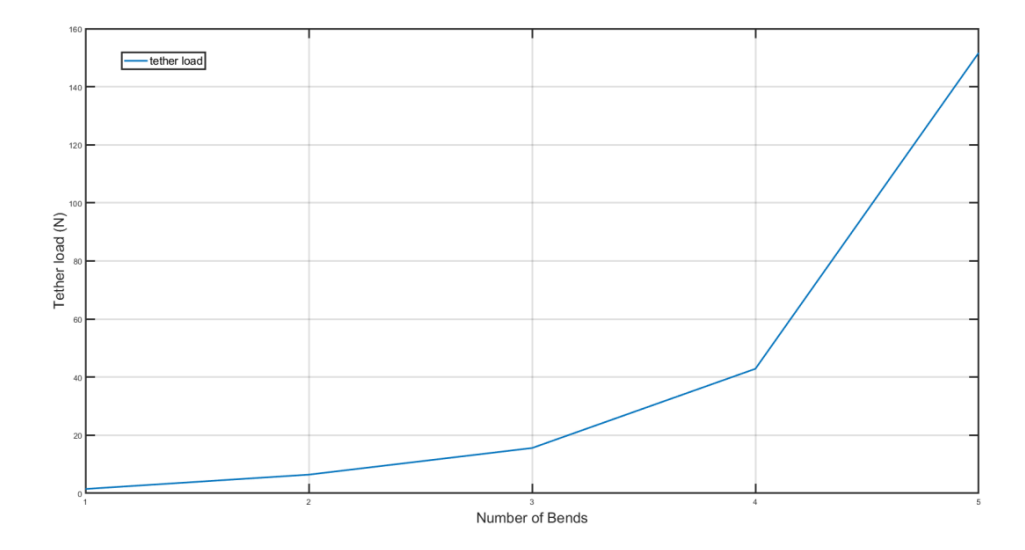


Figure 17 - Tether load.

To improve the ability for the crawler to navigate longer pipe lengths, a second crawler was developed and coupled with the first crawler to assist in distributing the tether load. Testing was then conducted with the two crawler system. It should be noted that multiple design iterations were made after the initial crawler tests were performed. The original prototypes for both the crawler and the inspection modules were 3D printed with white tough PLA, ABS, and polycarbonate. While the newer prototypes in the following images appear to be black as they were 3D printed with black tough PLA.

Both crawlers are identical in design and in length. In addition, a second electronics module was built to house the same electronic components and communicate with the first crawler. The tether is firmly attached to the external body of these modules but is internally connected by plastic wire connectors directly to the printed circuit boards. The system was originally designed to be modular so that quick individual changes or reprogramming the microcontrollers can be made to the system.

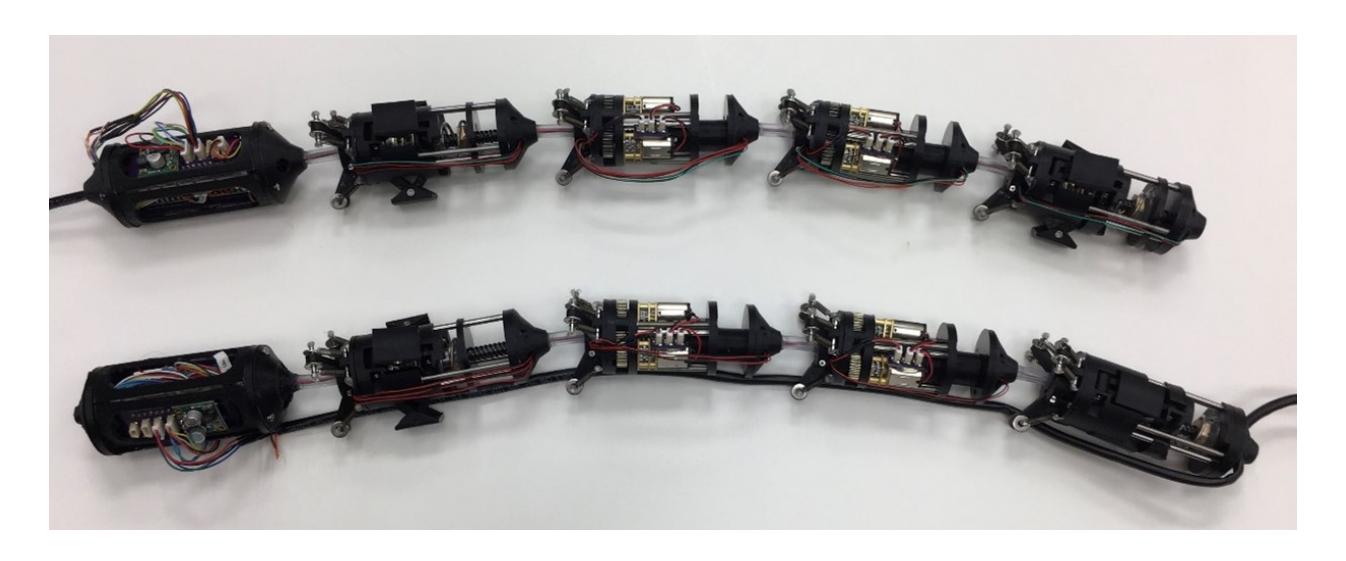


Figure 18 - Duplicate crawler units.

The crawlers were tethered together approximately 23.3 feet apart; this distance is equivalent to 4 bends to properly distribute the load. The tether behind the second crawler was measured to be the entire length of the mockup to be able to navigate the rest of the mockup on its own. Multiple tests were conducted to assess the system's ability to travel through bends and straight sections simultaneously. In the figure below, the first crawler was able to successfully navigate a straight section while the second crawler approached a bend. By the time it passed this bend, the first crawler reached the following bend. Thus, both units work in tandem to distribute the load as they alternate traveling through 180 degrees.

It was anticipated that the control strategy for moving both crawlers was especially important when traveling through bends. Thus, the serial communication system that was developed was used to command each crawler individually such as halting crawler 1 while moving crawler 2 forward, or moving crawler 1 forward while moving crawler 2 backward, etc. Each command was sent individually through the tether line via the master microcontrollers' serial monitor.

Judgment to halt or change the direction of the crawlers together, was made visually since this was a clear plastic mockup. However, to equip the system for inspection in metal superheater tubes, future efforts will be made to implement a means to measure the tether load at the front and back ends of both crawlers. The team has considered options such as an external force transducer or strain gauge attached to the junction where the ethernet cable tether meets the crawler module end caps.

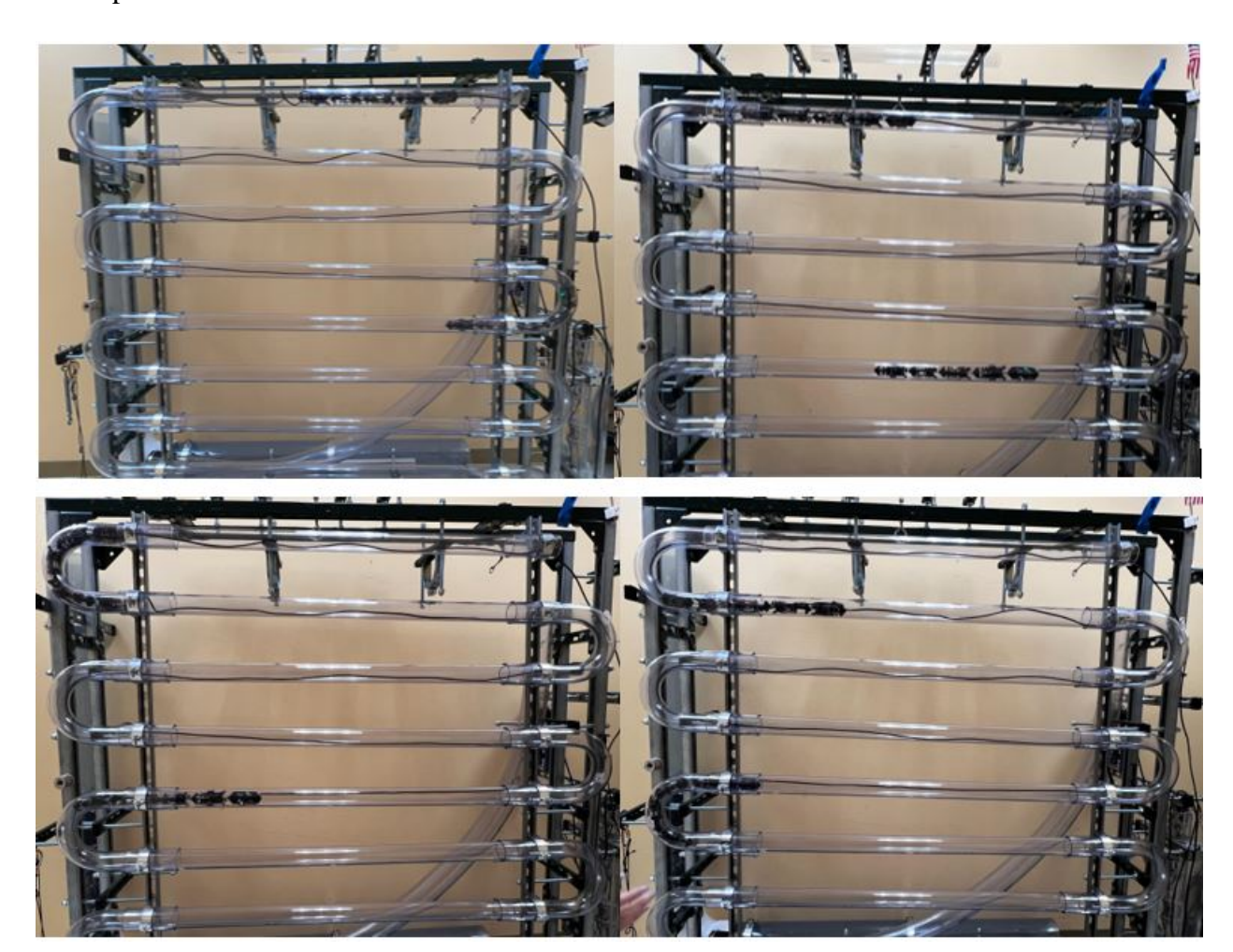


Figure 19 - Engineering scale testing of both crawlers navigating the superheater tube mockup.

2.5 Simulation Model Development

The development of the crawler significantly depended on the coil geometry of the tubes/pipes. In an initial geometric analysis, efforts were made to design the system to be capable of navigating through 5 cm radius bends. This led to the modules having a maximum diameter of 3.5 cm and a maximum length of 7 cm.

To improve the design of the peristaltic crawler and set the framework to evaluate the controls of the system, a high-fidelity model has been developed. Figure 20 shows a detailed schematic of the gripper and extender modules and includes key components and dimensions. The

gripper module consists of a total of 31 bodies and uses 14 joints to incorporate the constraints needed to generate the required motion. In addition, 16 constraints are used to implement limitations on the motion. The bodies include two end caps that can be used to mount the flexible cable connecting the modules, a lead screw, a lead nut and a helical spring. Additionally, there are 9 links connecting the spring and the bottom end caps that support the gripper pad with a revolute joint. This joint provides the constraints so that the pads can contact the internal pipe surface, regardless of the orientation of the linkage. A micro-gear motor is used to rotate the lead screw and expand the linkages that mate the pads with the pipe surface. Similarly, the extender consists of 22 bodies and uses 8 joints to generate the motion. However, only 1 motion constraint is required which limits the module's extension distance. Two micro-gear motors are used in the extender to provide the necessary torque on the lead screw that extends the top of the module. The stroke length for each module is approximately 2.58 cm, resulting in 5.16 cm of displacement for each cycle of the crawler.

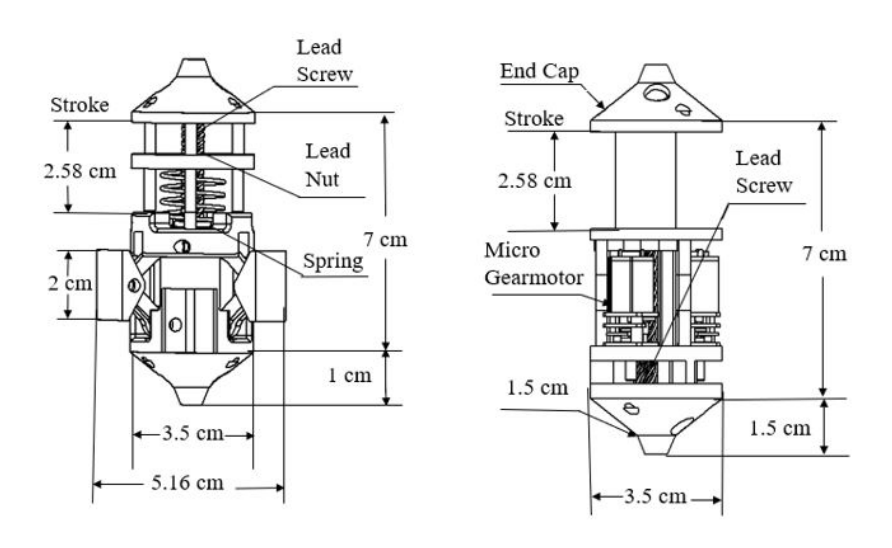


Figure 20 - Schematic of the gripper and extender modules.

To generate peristaltic motion of the crawler, the gripper in the rear extends and fixes its position within the tube while the other modules are collapsed. With the rear gripper position fixed, the two extenders simultaneously extend, moving the front gripper forward 5.16 cm. The front gripper then extends, fixing its position within the tube, and the rear gripper collapses. The two

extenders then retract pulling the rear gripper forward 5.16 cm. The cycle generates 5.16 cm of motion for the crawler and is repeated continuously until the crawler reaches its destination.

In addition, a simplified force analysis of a single gripper and extender in a static state was conducted. The gripper must be capable of generating a friction force greater than the drag force generated from the tether. If the friction force is lower than the drag force, the gripper will slip backwards. Similarly, when the extender is retracting, it must be capable of overcoming the tether load, or there would be no motion generated.

A simulation of the gripper and extender was created using a Solidworks motion simulation package. The analysis included extending one gripper that was resting on the bottom of a 5 cm tube. A motor drives the lead screw which extends the gripper arms until the three pads reach the inner wall of the tube, as shown in Figure 21.

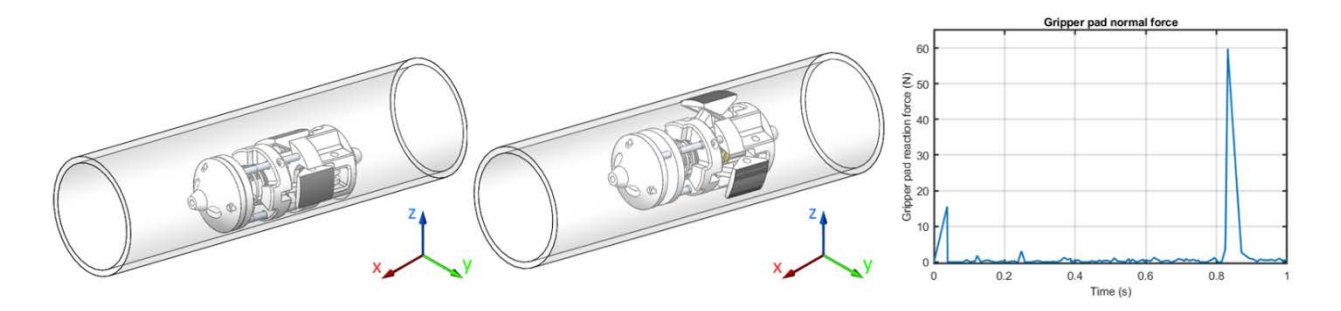


Figure 21 - Motion analysis of the gripper.

The normal force produced from the simulation is also shown in Figure 21. A peak force of approximately 60 N was obtained for one gripper. The result also shows smaller peaks in the normal force as the linkage arms extend. These peaks were due to the weight of the gripper on the lower arm. The friction force generated by the gripper is dependent on the normal force and the coefficient of friction between the pad and tube wall. For this analysis, a coefficient of friction of 0.6 was used for the interface between the rubber pad and steel tube surface. This was experimentally determined in accordance with ASTM D1894 [23] and agrees with standard values provided in the literature. This provides a maximum static friction force of 36 N per pad. With the three pads, this results in a simulated force of 108 N.

Additional data from the gripper simulation shows the axial motion of the lead screw, the radial displacement of the arm linkage, and the radial displacement of the gripper pad (Figure 22).

The simulation was conducted from the closed position to the extended position. As the nut is moved forward, the angle of the linkages changes and moves the gripper pad towards the inner surface of the pipe.

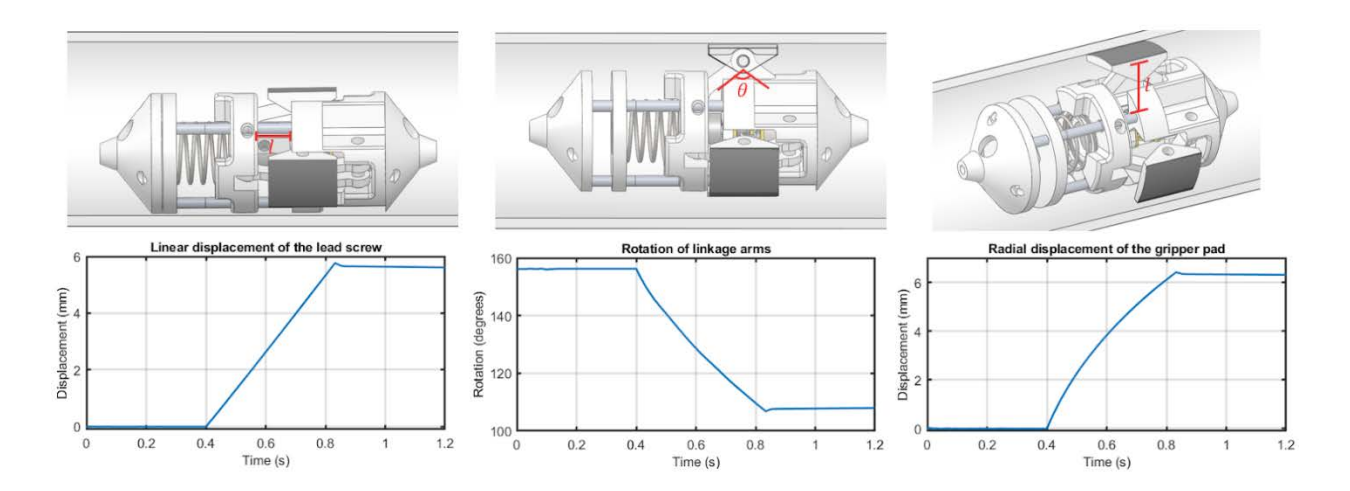


Figure 22 - Gripper component motion.

A simulation was also conducted on the extender module. Similar to the gripper, a motor drives a lead screw, causing the lead nut to extend toward the module's end cap. The maximum extension of the module is 2.58 cm.

2.6 Simulation in ADAMS

After developing a basic motion study in SOLIDWORKS, efforts were switched to MSC ADAMS (a Multibody Dynamic Simulation Software) to develop high-fidelity virtual simulations. ADAMS provides a larger database of tools and functionality which will be useful in developing a control strategy for the high-fidelity simulation. ADAMS also provides the ability to conduct design optimization studies that can be used during the motion analysis to optimize the simulation results. A dynamic motion simulation has been performed by importing the 3D CAD model of the gripper in ADAMS. All the constraints were assigned to each body of the gripper. This dynamic motion analysis provides a contact force of approximately 42N in each gripper pad with a friction force of 126N between the gripper and the 50mm tube.

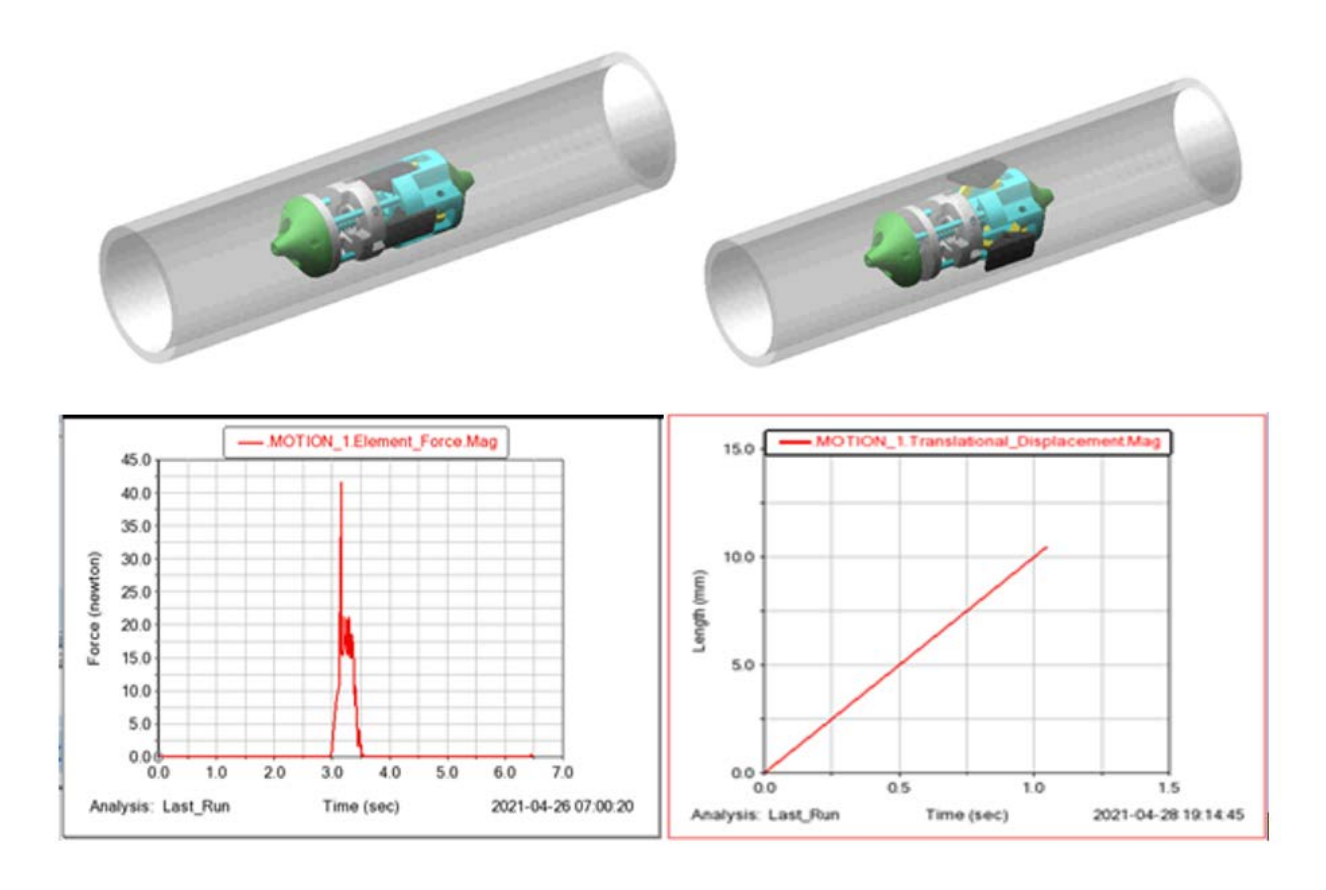


Figure 23 - Motion analysis of gripper module in ADAMS.

Motion analysis was also conducted for the extenders that are connected between the front and rear grippers. In this analysis, efforts were made to find the maximum displacement an extender can travel for a complete single extension and the operating speed at which the extender extends. The extension/retraction of the extenders occurs after either the rear gripper or front gripper engages the pipe wall. This conducted simulation provides a maximum displacement of 25 mm approximately and the operating speed is 10 mm/sec.

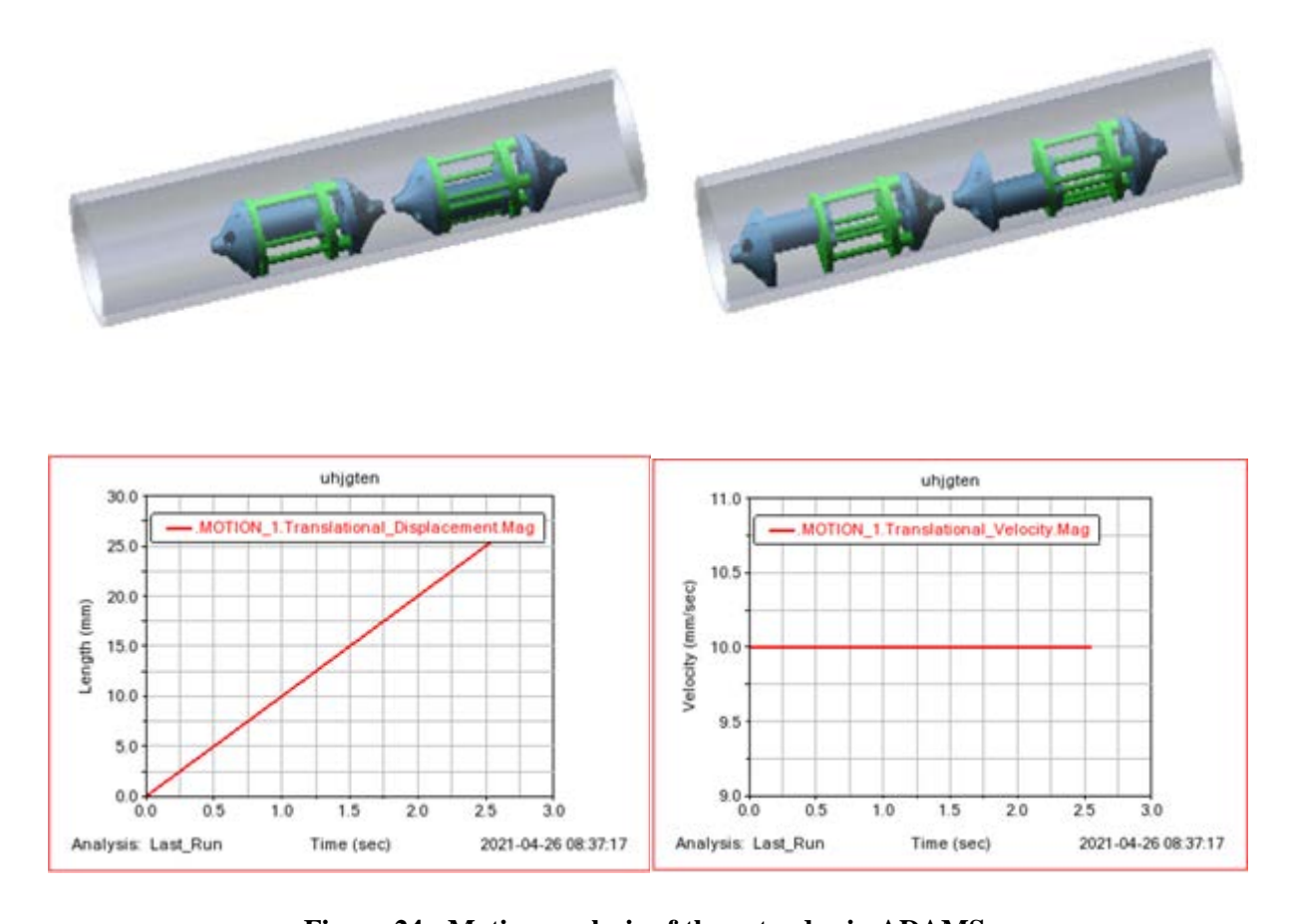


Figure 24 - Motion analysis of the extender in ADAMS.

After developing the motion analysis of the gripper and extender individually, efforts were made to generate a high-fidelity virtual simulation of the pipe crawler including all modules. Creating a simulation of a system provides a platform to evaluate designs virtually, reducing costs and saving time developing prototypes. Ultimately, the simulation will include load inputs from the motors and the outputs will include the speed of the system and its pull force.

For this process, CAD models of the gripper and extender modules were designed in SOLIDWORKS and exported as Parasolid files to a multibody simulation software. Next, the geometry of the bodies were defined and joints were added between the bodies that provide required motion and define the kinematics of the system. These joints include revolute, fixed, and prismatic joints. In addition to defining body geometry and joints, the material characteristics were

defined, that included density and inertia properties. At this phase of the model development, forward and reverse position motions were prescribed with the prismatic joints associated with the screw/nut system. In the future, forces equivalent to those created by the motor will be used to propel the system.

Each gripper module includes one prismatic joint and 16 revolute joints, while the extenders have only one prismatic joint. This prismatic joint provides the degree-of-freedom (DOF) for forward and reverse motion of the system. Between each module, a spherical joint is inserted to provide the relative motion between the modules. This joint allows for the rotational motion needed to navigate through bends in the pipes. Rotational stiffness is also added via a spring element. Note that careful attention needs to be paid to accurately represent this stiffness. Furthermore, each of the bodies have a contact element that generates a force between the body element and the pipe.

The motion simulation of the pipe crawler system was carried out by varying the contact parameters between the colliding bodies of the modules and the pipe. Efforts were made to represent the navigation accurately without significantly increasing the computational time. Numerical drift has been considerably reduced by investigating the contact parameters of the system. The large number of collisions between the modules and the pipe makes it difficult for the software to numerically solve the equations of motion, resulting in computationally expensive simulations. Figure 25 shows the crawler navigating through the straight sections and bends.

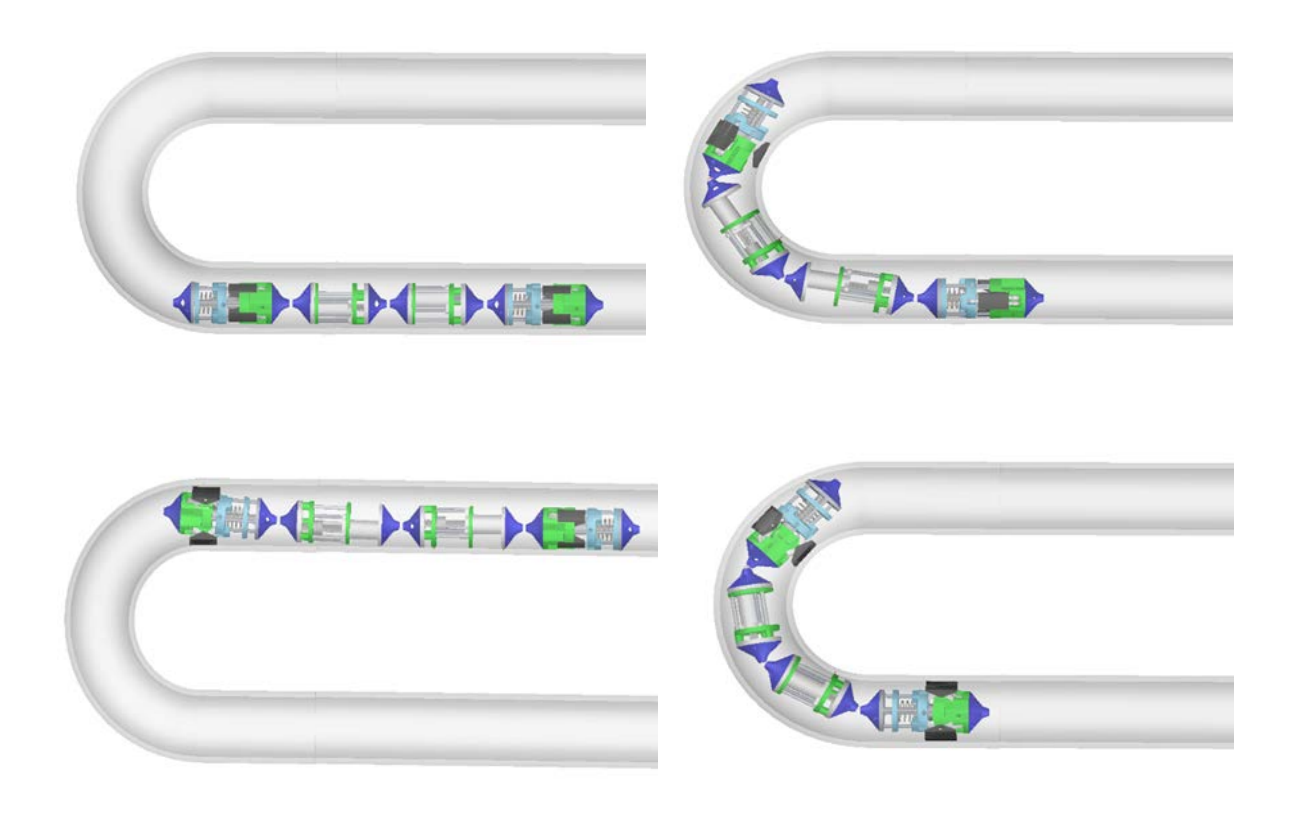


Figure 25 - Motion simulation of the crawler through the straight sections and bends of the pipe.

The primary objectives of this task is to develop a high-fidelity simulation of the system with a realistic pull force result similar to those obtained via the crawler's experimental testing. Accurate contact parameters between the colliding bodies provide the contact force that aids in determining the true pull force of the system. During the motion simulation of the crawler, contact forces between the gripper pad and the pipe were investigated. Figure 26 shows the normal force of the gripper pad while it engages the pipe wall.

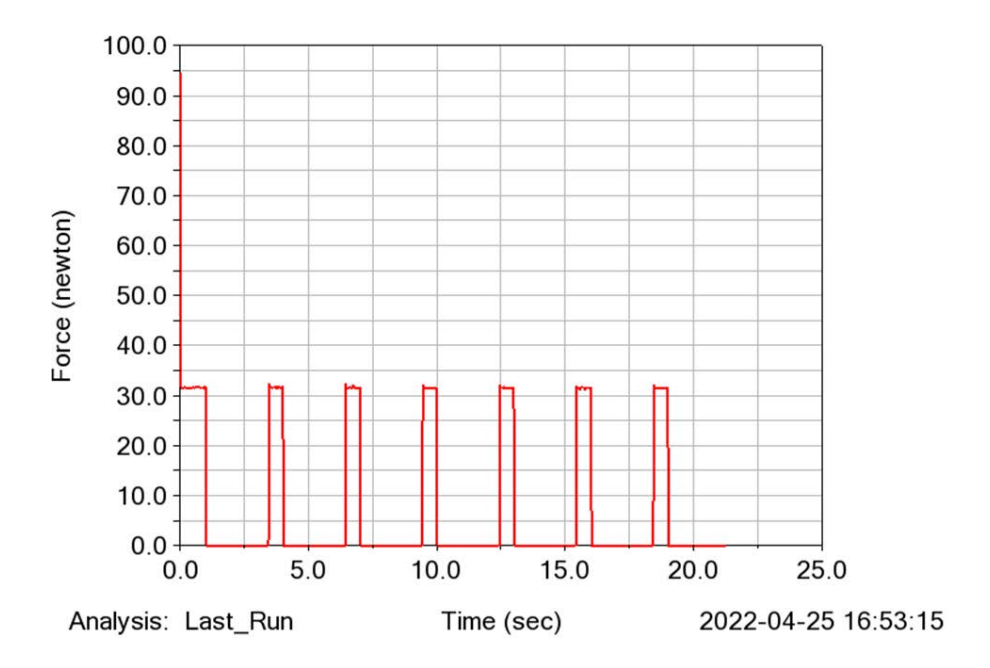


Figure 26 - Normal force between the gripper pad and the pipe.

The contact force obtained for each gripper pad of the module is approximately 32 N. With the appropriate coefficient of friction of the material used for the simulation, this contact force creates a friction force that complies with the pull force of the system found in the engineering scale tests.

After evaluation of a single crawler, the study was continued by conducting a simulation of two pipe crawlers navigating in a virtual mockup, simultaneously. Developing a body to represent the tether connecting the crawlers is not possible in ADAMS, however, a force representing the tether force between the two crawlers can be added. Initial efforts focused on understanding the challenges with the software with the addition of the second crawler. Simulations demonstrated that we were able to achieve a significant reduction in the computational time while navigating through the straight sections by properly defining contact parameters. However, there are still challenges associated with navigating through the elbows, due the complex motion and contact between the crawler and the pipe.

Prior to conducting the simulation of two crawlers, all the necessary geometrical constraints analogous to the first crawler were applied. Both crawlers navigate well in the straight

sections but computationally stall in some intervals of the bends. Figure 27 represents a portion of a transparent mockup that carries two pipe crawlers simultaneously.

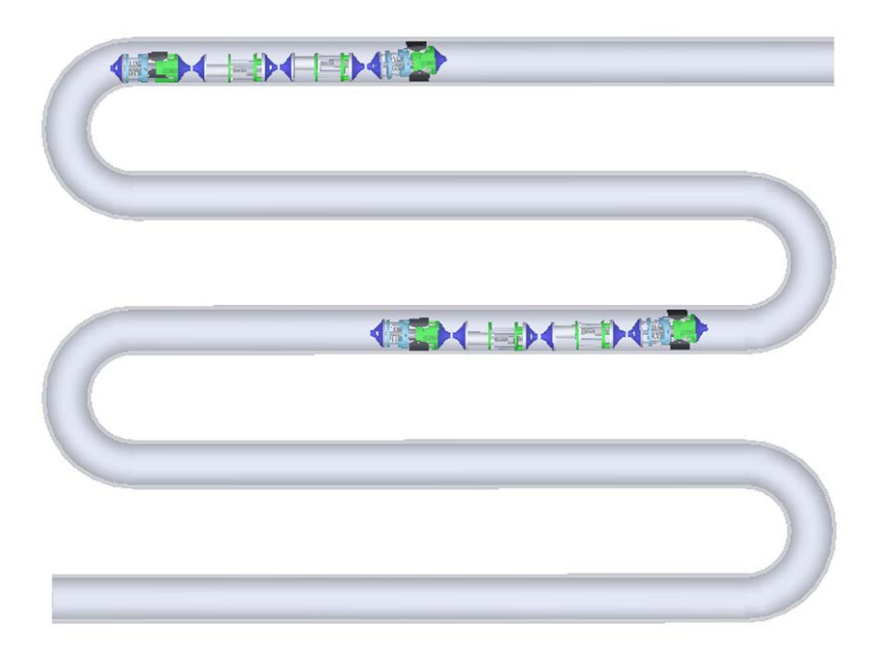


Figure 27 - Motion simulation of two crawlers navigating in the pipe simultaneously.

Efforts are continuing to understand the challenges of conducting the multi crawler simulation through the elbows. This includes altering contact parameters to reduce the numerical drift and computational time. We are also continuing to develop a controller for the multi crawler system using MATLAB/Simulink. Simulation results of pull force from ADAMS are the inputs to the Simulink controller. Outputs of the controller are returned to ADAMS to control the speed and motion of the system.

3. CONCLUSIONS

A robotic multi-crawler system has been developed that can navigate through 5 cm diameter tubes similar to those found in fossil energy power plants. The base modules for navigation include two grippers and two extenders. The maximum pull force of the system is limited by the strength of the extenders which is 40 N. When the drag force of the tether reached this value, an additional crawler was inserted to assist in the load distribution. Additional modules have been developed that include an electronics module, a UT sensor module, a surface preparation

module, and an instrumentation module. Testing of the crawler system demonstrates its ability to

navigate through multiple straight sections and 180° bends. Initial testing of the modules

demonstrated the system's ability to inspect the integrity and conditions within 5 cm diameter

tubes.

Several issues were investigated in efforts to improve the performance of the system. Since

the distance the crawler can navigate is limited by its pull force capability, efforts were made to

improve the extenders and grippers and reduce the drag on the system. Design modifications were

done including incorporation of the stabilization mechanism in the gripper and extender modules

to reduce drag and improve the performance in elbows. Efforts were also made to improve the

wire management by incorporating slip rings in the rotating modules.

Future aspects that can continue to be investigated is the development of a control box to

manage and collect data from the camera and sensors. Software and hardware will need to be

developed for the data management manage and improve the TRL of the system. Engineering-

scale testing with the control box would further improve the TRL.

In this study, integration of the sensors in the instrumentation module was conducted with

basic sensors that were commercially available off-the-shelf. Future efforts could also include

improving the accuracy and resolution of the sensors by developing custom designed sensors with

improved performance.

The high-fidelity simulation model can also continue to be developed and improved.

Accurate models of each module have been integrated together and provide a platform for

developing a virtual environment for evaluation of the system. This will allow for the assessment

of module design changes, system additions to augment the crawler's functionality, and control

strategies to maximize the performance of the system.

4. PARTICIPANTS AND OTHER COLLABORATING ORGANIZATIONS

This research effort is conducted by the PI, Co-PI, Research Scientist, graduate student and

undergraduate student. The roles of each person are described below.

Name: Dwayne McDaniel, Ph.D., P.E.

Project Role: PI

Contribution to Project: Management of all technical and fiscal aspects of the project.

Name: Aparna Aravelli, Ph.D.

Project Role: Co-PI

Contribution to Project: Assist in the management of the project and direct technical aspects with related

to the sensors.

Name: Anthony Abrahao

Project Role: Research Scientist (and Ph.D. Candidate)

Contribution to Project: Leads the efforts associated with the development of the crawler including

design, manufacturing and testing

Name: Sharif Sarker

Project Role: Doctoral Student – Mechanical Engineering

Contribution to Project: Supports the team in developing a high-fidelity model of the crawler with will be

used to evaluate control methods to maximize the capability of the crawler.

Name: Caique Lara

Project Role: Masters Student – Mechanical Engineering

Contribution to Project: Supports Dr. Aravelli in the selection, testing and integration of the sensors.

Name: Julie Villamil

Project Role: Undergraduate Student – Mechanical Engineering

Contribution to Project: Supports Mr. Abrahao in the development and testing of the crawler.

5. REFERENCES

- 1. F. Dehnavi, A. Eslami, and F. Ashrafizadeh, "A case study on failure of superheater in an industrial power plant", Engineering Failure Analysis 80, 368–377 (2017).
- 2. G. J. Abraham, V. Kain, and N. Kumar, "Cracking of superheater tube in a captive power plant", Corrosion Engineering Science and Technology 53, 98–104 (2018).
- 3. A. Nayak and S. K. Pradhan, "Design of a new in-pipe inspection robot", Procedia Engineering 97, 2081–2091 (2014).
- 4. S. D. Kapayeva, M. J. Bergander, A. Vakhguelt, and S. I. Khairaliyev, "Remaining life assessment for boiler tubes affected by combined effect of wall thinning and overheating", Journal of Vibroengineering 19, 5892–5907 (2017).
- 5. J. Shang, B. Bridge, T. Sattar, S. Mondal, and A. Brenner, "Development of a climbing robot for inspection of long weld lines", Industrial Robot 35, 217–223 (2008).
- 6. C. Balaguer, A. Gim'enez, J. M. Pastor, V. M. Padr'on, and M. Abderrahim, "Climbing autonomous robot for inspection applications in 3D complex environments", Robotica 18, 287–297 (2000).
- 7. G. La Rosa, M. Messina, G. Muscato, and R. Sinatra, "A low-cost lightweight climbing robot for the inspection of vertical surfaces", Mechatronics 12, 71–96 (2002).

- 8. D. Longo and G. Muscato, "A modular approach for the design of the Alicia3 climbing robot for industrial inspection", Industrial Robot 31, 148–158 (2004).
- 9. M. Tavakoli, C. Viegas, L. Marques, J. N. Pires, and A. T. De Almeida, "OmniClimbers: Omnidirectional magnetic wheeled climbing robots for inspection of ferromagnetic structures", Robotics and Autonomous Systems 61, 997–1007 (2013).
- 10. P. Sangdeok, D. J. Hee, and S. L. Zhong, "Development of mobile robot systems for automatic diagnosis of boiler tubes in fossil power plants and large size pipelines", in Proceedings ieee/rsj international conference on intelligent robots and systems (2002).
- 11. A. Hadi, A. Hassani, K. Alipour, R. Askari Moghadam, and P. Pourakbarian Niaz, "Developing an adaptable pipe inspection robot using shape memory alloy actuators", Journal of Intelligent Material Systems and Structures 31, 632–647 (2020).
- 12. T. Kishi, M. Ikeuchi, and T. Nakamura, "Development of a Peristaltic Crawling Inspection Robot for Half-Inch Pipes Using Pneumatic Artificial Muscles", SICE Journal of Control, Measurement, and System Integration 8, 256–264 (2015).
- 13. S. Tesen, N. Saga, T. Satoh, and J. ya Nagase, "Peristaltic Crawling Robot for Use on the Ground and in Plumbing Pipes", CISM International Centre for Mechanical Sciences, Courses and Lectures 544, 267–274 (2013).
- 14. H. Omori, T. Nakamura, and T. Yada, "An underground explorer robot based on peristaltic crawling of earthworms", Industrial Robot 36, 358–364 (2009).
- 15. P. Debenest, M. Guarnieri, and S. Hirose, "Pipe Tron Series-Robots for pipe inspection", Proceedings of the 3rd International Conference on Applied Robotics for the Power Industry, CARPI 2014, 10.1109/CARPI. 2014.7030052 (2015).
- 16. J. Y. Nagase, K. Suzumori, and N. Saga, "Development of worm-rack driven cylindrical crawler unit", Journal of Advanced Mechanical Design, Systems and Manufacturing 7, 422–431 (2013).
- 17. F. Ito, T. Kawaguchi, Y. Yamada, and T. Nakamura, "Development of a peristaltic-movement duct-cleaning robot for application to actual environment examination of brush type and installation method to improve cleaning efficiency", Journal of Robotics and Mechatronics 31, 781–793 (2019).
- 18. A. A. Gargade and D. S. S. Ohol, "Development of In-pipe Inspection Robot", IOSR Journal of Mechanical and Civil Engineering 13, 64–72 (2016).
- 19. A. S. Boxerbaum, K. M. Shaw, H. J. Chiel, and R. D. Quinn, "Continuous wave peristaltic motion in a robot", International Journal of Robotics Research 31, 302–318 (2012).
- 20. J. Qiao, J. Shang, and A. Goldenberg, "Development of inchworm in-pipe robot based on self-locking mechanism", IEEE/ASME Transactions on Mechatronics 18, 799–806 (2013).
- 21. H.- J. Yeo, "Development of a Robot System for Repairing a Underground Pipe", Journal of the Korea Academia-Industrial cooperation Society 13, 1270–1274 (2012).

- 22. J. Y. Nagase, F. Fukunaga, and Y. Shigemoto, "Cylindrical elastic crawler mechanism for pipe inspection", Advances in Cooperative Robotics: Proceedings of the 19th International Conference on Climbing and Walking Robots and the Support Technologies for Mobile Machines, CLAWAR 2016, 304–311 (2016).
- 23. Standard test method for static and kinetic coefficients of friction of plastic film and sheeting, https://www.astm.org/Standards/D1894.htm, [Online; accessed 11-March-2021].